Journal of Molecular Catalysis A: Chemical 328 (2010) 68–75

Contents lists available at ScienceDirect

Journal of Molecular Catalysis A: Chemical

journal homepage: www.elsevier.com/locate/molcata

Modular chiral diphosphite derived from L-tartaric acid. Applications in metal-catalyzed asymmetric reactions

Alonso Rosas-Hernández[a], Edgar Vargas-Malvaez[a], Erika Martin[a,*], Laura Crespi[b], J. Carles Bayón[b]

[a] Departamento de Química Inorgánica, Facultad de Química, Universidad Nacional Autónoma de México, México DF 04510, Mexico
[b] Departament de Química, Universitat Autònoma de Barcelona, Bellaterra 08193, Barcelona, Spain

ARTICLE INFO

Article history:
Received 16 December 2009
Received in revised form 19 May 2010
Accepted 1 June 2010
Available online 8 June 2010

Keywords:
Asymmetric catalysis
Chiral diphosphite
Hydroformylation
Allylic alkylation

ABSTRACT

A new family of C_2-symmetric chiral diphosphites was synthesized using two different chiral backbones derived from tartaric acid, combined with chiral binaphthyls or non-chiral substituted biphenyl moieties. Diphosphites were applied to Rh-catalyzed hydroformylation of styrene producing good conversions in mild conditions, fair regioselectivities but low enantioselectivities in all cases. Ligands were also essayed in Pd-catalyzed allylic substitution reactions of linear and cyclic substrates using dimethyl malonate as nucleophile. Conversion rates up to 7200 h^{-1} were reached, while moderated ee's were attained. In this reaction, a kinetic resolution of *rac*-1,3-diphenyl-3-acetoxyprop-1-ene was observed, leading to 99% ee of for the unreacted *S*-substrate and 60% ee of *S*-alkylated product. Coordination properties of diphosphites in rhodium and palladium complexes related to catalytic species involved in the two previous reactions were investigated. Some ligands form equatorial-equatorial chelates in pentacoordinated complexes [RhH(CO)(PPh_3)(diphosphite)], while other act as bridge between two metal atoms. In the catalytic active species [Pd(η^3-PhCHCHCHPh)(diphosphite)]PF_6 one or two diastereoisomers are formed, depending on the diphosphite structure.

1. Introduction

The development of asymmetric transition-metal catalysis depends on the availability of enantiomerically pure ligands. Among them, chiral diphosphites are especially attractive because their structural properties can be easily modified allowing a fine-tuning of the performance of the corresponding metal catalyst [1]. Since chiral diphosphites are readily prepared from a diol backbone and an appropriate phosphorochloridite, a great variety of these ligands have been described generating libraries in which both, electronic and steric properties are systematically modified. These libraries have been very often screened in hydroformylation and allylic substitution reactions [2,3].

Asymmetric rhodium-catalyzed hydroformylation using diphosphites derived from chiral alkyl-diol backbones was initially explored by Babin and Whiteker [4] and later by van Leeuwen and coworkers [5]. High enantioselectivities were achieved in the hydroformylation of vinylarenes with Chiraphite, a ligand derived from (2*R*,4*R*)-pentanediol, but similar diphosphites based on shorter or longer alkyl backbones, render poorly enantioselective catalysts. This difference has been attributed to the ability of Chiraphite to form *bis*-equatorial chelate in [RhH($CO)_2$(diphosphite)] catalytically active species. As (*R*,*R*)-Chiraphite, sugar-based diphosphites producing good enantioselectivities form eight-membered chelate rings when they coordinate to the metal center [6,7]. In contrast, (*S*,*S*)-Kelliphite, one of the most efficient ligands for asymmetric hydroformylation forms a nine-membered metal chelate [2,8]. Moreover, it has been shown that a diphosphite forming 16-membered chelate ring is able to produce fair asymmetric induction in the hydroformylation of vinylarenes [9].

Since the beginning of this decade, reports on the application of chiral diphosphites to the allylic substitution reaction have greatly increased [10–19]. Most of the new ligands synthesized have been tested in alkylation of *rac*-1,3-diphenyl-3-acetoxy-1-ene, which often gave better enantioselectivities than unsymmetrically substituted or less-sterically demanding allylic substrates. It should be noted that (*R*,*R*)-Chiraphite and sugar-based diphosphites that perform well in asymmetric hydroformylation are among the best ligands for the alkylation of *rac*-1,3-diphenyl-3-acetoxy-1-ene [13,14]. These type of ligands produced ee's near to 95%, with high turnover frequencies (>2000 h^{-1}). Even higher rates and 98% ee, were achieved in the same reaction using a C_2 diphosphite, containing bulky silyl substituents on furanoside backbone [15] however; this ligand produces poor stereoselectivity in the rhodium-catalyzed styrene hydroformylation [20].

With the aim to get further insight into the relation between the structure of diphosphites and their catalytic performance, we report here a new family of these ligands (Scheme 1) and their

* Corresponding author. Tel.: +52 55 56223720; fax: +52 55 56223720.
E-mail address: erikam@unam.mx (E. Martin).

1381-1169/$ – see front matter © 2010 Elsevier B.V. All rights reserved.
doi:10.1016/j.molcata.2010.06.001

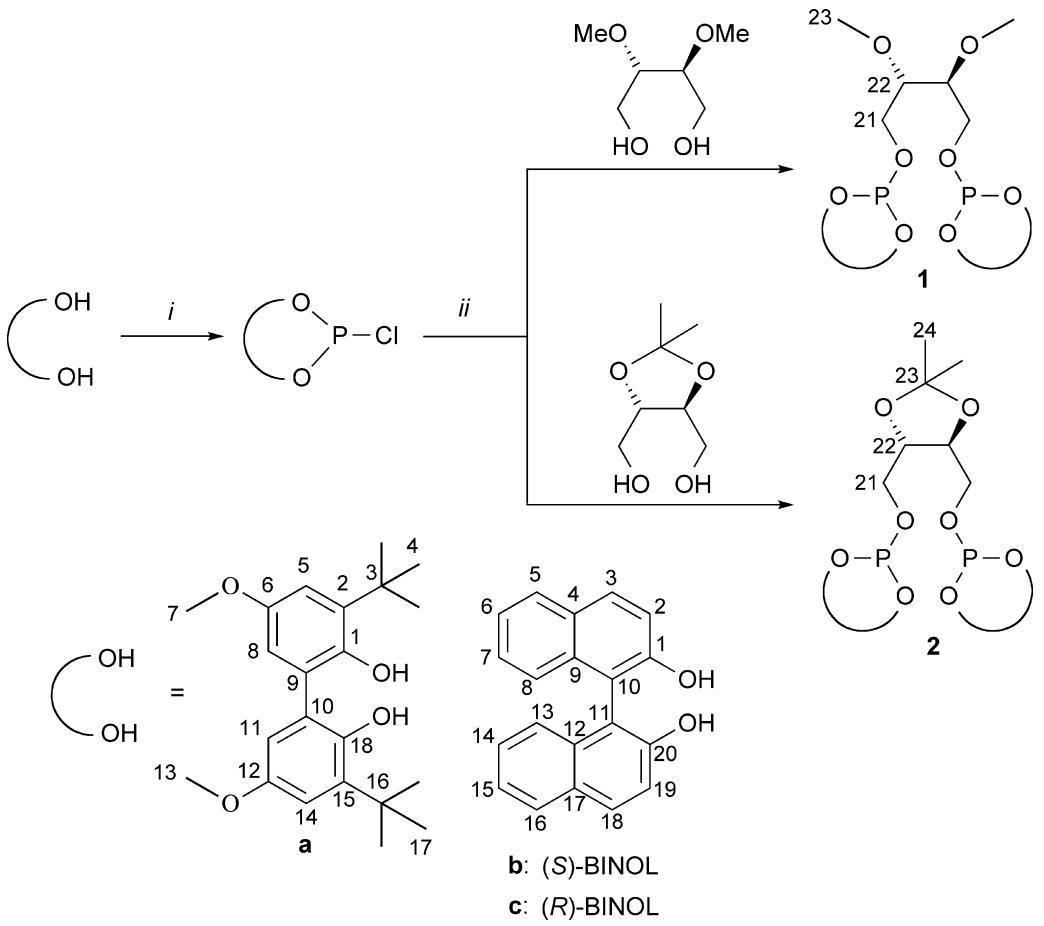

Scheme 1. Syntheses of chiral diphosphite ligands **1**-**2**. (i) PCl_3, NEt_3, THF, −40 °C to 20 °C, 4 h; (ii) NEt_3, THF, −40 °C to 20 °C, 18 h.

catalytic screening in hydroformylation and allylic alkylation reactions. The backbone of these diphosphites was built from tartaric acid, a natural and readily available chiral source. Ligands **2b** and **2c**, bearing four carbon atoms at the backbone, with some restricted flexibility imposed by the 1,3-dioxolane fragment, and atropoisomeric phosphite moieties, could mimic the conformational constrains of Kelliphite. For comparative purposes, ligand **2a**, with a non-chiral fragment as terminal phosphorous substituents, has also been synthesized. The homologous series of ligands **1a**–**c**, in which the stiffness of the four carbon atoms backbone has been released, is also studied.

2. Experimental

2.1. General methods

All reactions were carried out under nitrogen atmosphere using standard Schlenk techniques. Solvents were dried by standard procedures. NEt_3 over KOH and PCl_3 and were distilled prior to use. Diols (2*S*,3*S*)-2,3-dimethoxy-1,4-butanediol [21,22], (4*S*,5*S*)-2,2-dimethyl-1,3-dioxolane-4,5-dimethanol [23] and 3,3′-di-*tert*-butyl-5,5′-dimethoxy-2,2′-biphenyldiol [24] were prepared according to literature procedures. Phosphorochloridite intermediates, 6-chloro-4,8-*bis*(1,1-dimethylethyl)-2,10-dimethoxy-dibenzo[d,f][1,3,2]dioxaphosphepine [25], and (*R*)- and (*S*)-(1,1′-binaphthalene-2,2′-dioxy)chlorophosphine [9] were prepared as previously described. Styrene (**S1**) was filtered through neutral activated alumina and substrates *rac*-1,3-diphenyl-3-acetoxyprop-1-ene (**S2**), 1-phenyl-3-acetoxyprop-1-ene (**S3**) and *rac*-3-acetoxycyclohexene (**S4**) were prepared following standard procedures [26]. The rest of reagents were from commercial origin and were used as received.

NMR spectra were recorded in *Bruker Avance-250, Varian Unity Inova-300, -400* and *Bruker ARX-400* instruments using $CDCl_3$ as solvent. Coupling constants are in hertz and chemical shifts are given in ppm referenced to solvent (^1H and ^{13}C) or external reference of 85% aqueous solution of H_3PO_4 (^{31}P). FAB^+ mass spectra were acquired in a Jeol SX102A spectrometer using 3-nitrobenzylalcohol matrix. High resolution TOF mass spectra were obtained by LC/MSD TOF on an Agilent Technologies equipment. Optical rotations were measured in a Perkin-Elmer 241 polarimeter, $[\alpha]^D$ values are in units of 10^{-1} deg cm^2 g^{-1}. Catalytic reaction mixtures were analyzed by GC-Varian 3800, GC-HP 5890 or HPLC Alliance-Waters chromatographs. Absolute configurations of chiral products were assigned by comparing their retention times with those of optically pure compounds. For further experimental details see supplementary data.

2.2. Syntheses of diphosphites: general method

To a solution containing 4.18 mmol of the (1,1′-biaryl-2,2′-dioxy)chlorodiphosphine and NEt_3 (2.28 g, 22.6 mmol) in THF (20 mL), 2.1 mmol of the corresponding diol in THF (5 ml) were slowly added at −40 °C. The mixture was allowed to reach room temperature and it was stirred overnight. The ammonium salt formed was filtrated over celite and the filtrate was evaporated to dryness. The solid residue was purified over silica using CH_2Cl_2 as eluent. The analytically pure products were recovered by evaporating the solvent, yielding white to slightly yellow powders (see Scheme 1 for the labeling used for NMR data).

(2S,3S)-2,3-dimethoxy-1,4-bis[(3,3′-di-tert-butyl-5,5′-dimethoxy-1,1′-bisphenyl-2,2′-diyl)phosphite]-butane **1a**. Yield 73%. ^{1}H NMR (300 MHz): 6.97 (d, 4H, H8, H11, $^{4}J_{H5\text{-}H8} = {}^{4}J_{H11\text{-}H14} = 3.17$), 6.70 (d, 4H, H5, H14, $^{4}J_{H5\text{-}H8} = {}^{4}J_{H11\text{-}H14} = 3.17$), 3.94–3.82 (m, 4H, H21), 3.81 (s, 12H, H7, H13), 3.52–3.33 (m, 2H, H22), 3.27 (s, 6H, H23), 1.54, 1.37 (2 s, 36H, H4, H17). ^{13}C{^{1}H} NMR (75.4 MHz): 155.8, 155.3 (4C, C6, C12); 142.4–141.9 (8C, C1, C18, C9, C10); 133.6–133.3 (4C, C2, C15); 114.5-114.0 (4C, C8, C11); 112.9–112.5 (4C, C5, C14); 79.2–78.9 (2C, C22); 62.3–62.0 (2C, C21); 59.1–58.9 (2C, C23); 55.9–55.3 (4C, C7, C13); 35.5–35.2 (4C, C3, C16); 32.5–29.3 (12C, C4, C17). ^{31}P{^{1}H} NMR (121.3 MHz): 132.9 (s). $[\alpha]_D{}^{25} = +15.82^\circ$ ($c = 1.24$, CH_2Cl_2). FAB$^+$ MS: *m*/*z*: 922 [M]$^+$. TOF MS: *m*/*z*: 945.4076 (Calcd. 945.4078 for $C_{50}H_{68}O_{12}NaP_2{}^+$), error (ppm) = −0.2393.

(2S,3S)-2,3-dimethoxy-1,4-bis[((S)-1,1′-binaphthyl-2,2′-diyl)phosphite]-butane **1b**. Yield 78%. ^{1}H NMR (300 MHz): 8.0–7.7, 7.5–7.0 (m, 24H, H2-H19), 4.10–3.70 (m, 4H, H21), 3.45–3.30 (m, 2H, H22), 3.24 (s, 6H, H23). ^{13}C{^{1}H} NMR (75.4 MHz): 148.5, 147.4 (2d, 4C, C1, C20, $^{2}J_{C\text{-}P} = 3.9$); 132.8, 132.6 (4C, C9, C12); 131.5, 131.0 (4C, C3, C18); 130.4, 130.1 (4C, C4, C17); 128.4, 128.3 (4C, C5, C16); 127.0, 126.9 (4C, C7, C14); 126.3, 126.2 (4C, C6, C15); 125.1, 124.9 (4C, C8, C13); 124.1, 122.6 (2d, 4C, C10, C11, $^{3}J_{C\text{-}P} = 3.9$); 121.8, 121.5 (2d, 4C, C2, C19, $^{3}J_{C\text{-}P} = 2.01$); 79.1 (d, 2C, C22, $^{3}J_{C\text{-}P} = 4.2$); 62.7 (d, 2C, C21, $^{2}J_{C\text{-}P} = 6.6$); 59.2 (2C, C23). ^{31}P{^{1}H} NMR (121.3 MHz): 141.9 (s). $[\alpha]_D{}^{25} = +413.41^\circ$ ($c = 1.23$, CH_2Cl_2). FAB$^+$ MS: *m*/*z*: 778 [M]$^+$. TOF MS: *m*/*z*: 801.1777 (Calcd. 801.1777 for $C_{46}H_{36}O_8NaP_2{}^+$), error (ppm) = −0.0829.

(2S,3S)-2,3-dimethoxy-1,4-bis[((R)-1,1′-binaphthyl-2,2′-diyl)phosphite]-butane **1c**. Yield 79%. ^{1}H NMR (250 MHz): 7.98–7.71, 7.49–6.95 (m, 24H, H2-H19), 4.08–3.81 (m, 4H, H21), 3.58–3.39 (m, 2H, H22), 3.24 (s, 6H, H23). ^{13}C{^{1}H} NMR (62.8 MHz): 153.2, 152.2 (4C, C1, C20). 133.9, 133.6 (4C, C9, C12); 131.7, 131.4 (4C, C3, C18); 130.1, 131.4 (4C, C4, C17); 129.0, 128.8 (4C, C5, C16); 127.8, 127.4 (4C, C7, C14); 126.9, 126.7 (4C, C6, C15); 125.5, 125.4 (4C, C8, C13); 124.7, 124.4 (4C, C10, C11); 118.7, 118.2 (4C, C2, C19); 79.7 (2C, C22); 62.1 (2C, C21); 60.1 (2C, C23). ^{31}P{^{1}H} NMR (101.3 MHz): 142.9 (s). $[\alpha]_D{}^{25} = -445.4^\circ$ ($c = 1.23$, CH_2Cl_2) FAB$^+$ MS: *m*/*z*: 779 [M+1]$^+$. TOF MS: *m*/*z*: 801.1777 (Calcd. 801.1777 for $C_{46}H_{36}O_8NaP_2{}^+$), error (ppm) = −0.0829.

(2S,3S)-2,3-O-isopropylidene-2,3-dihydroxy-1,4-bis[(3,3′-di-tert-butyl-5,5′-dimethoxy-1,1′-bisphenyl-2,2′-diyl)phosphite]-butane **2a**. Yield 90%. ^{1}H NMR (300 MHz): 7.00–6.93 (m, 4H, H8, H11); 6.72–6.65 (4H, H5, H14); 4.17–3.63 (m, 6H, H21, H22); 3.81 (s, 12H, H7, H13); 1.48, 1.34 (2 s, 36H, H4, H17); 1.32 (s, 6H, H23). ^{13}C{^{1}H} NMR (75.4 MHz): 155.7–155.3 (4C, C6, C12); 142.5–141.8 (8C, C1, C18, C9, C10); 133.7–133.2 (4C, C2, C15); 114.7–114.0 (4C, C8, C11); 113.1–112.3 (4C, C5, C14); 109.7–109.8 (1C, C23); 76.9–76.7 (2C, C22); 64.4–64.1 (2C, C21); 55.8–55.3 (4C, C7, C13); 35.5–35.1 (4C, C3, C16); 31.4–30.0 (12C, C4, C17); 27.3–26.6 (2C, C24). ^{31}P{^{1}H} NMR (121.3 MHz): 129.5 (s). $[\alpha]_D{}^{25} = -32.93^\circ$ ($c = 1.26$, CH_2Cl_2) FAB$^+$ MS: *m*/*z*: 935 [M+1]$^+$. TOF MS: *m*/*z*: 935.4255 (Calcd. 935.4258 for $C_{51}H_{69}O_{12}P_2{}^+$), error (ppm) = −0.4080.

(2S,3S)-2,3-O-isopropyliden-2,3-dihydroxy-1,4-bis[((S)-1,1′-binaphthyl-2,2′-diyl)phosphite]-butane **2b**. Yield 73%. ^{1}H NMR (300 MHz): 8.00–7.70, 7.56–7.10 (m, 24 H, H2-H19), 4.07–3.80 (m, 2H, H22), 3.80–3.65 (m, 4H, H21), 1.33 (s, 6H, H24). ^{13}C{^{1}H} NMR (75.4 MHz): 148.7, 147.3 (2d, 4C, C1, C20, $^{2}J_{C\text{-}P} = 4.2$); 132.8, 132.6 (4C, C9, C12); 131.6, 131.0 (4C, C3, C18); 130.5; 130.9 (4C, C4, C17); 128.4, 128.3 (4C, C5, C16); 127.0, 127.0 (4C, C7, C14); 126.3, 126.3 (4C, C6, C15); 125.1, 124.9 (4C, C8, C13); 124.0, 122.6 (2d, 4C, C10, C11, $^{3}J_{C\text{-}P} = 4.0$); 121.8, 121.5 (2d, 4C, C2, C19, $^{3}J_{C\text{-}P} = 2.2$); 110.1 (1C, C23); 76.4 (d, 2C, C22, $^{3}J_{C\text{-}P} = 3.8$); 64.1 (d, 4C, C21, $^{2}J_{C\text{-}P} = 3.6$); 27.1 (6C, C24). ^{31}P{^{1}H} NMR (121.3 MHz): 134.3 (s). $[\alpha]_D{}^{25} = +429.03^\circ$ ($c = 1.24$, CH_2Cl_2) FAB$^+$ MS: *m*/*z*: 791 [M+1]$^+$. TOF MS: *m*/*z*: 791.1959 (Calcd. 791.1959 for $C_{47}H_{37}O_8P_2{}^+$), error (ppm) = 0.0988.

(2S,3S)-2,3-O-isopropyliden-2,3-dihydroxy-1,4-bis[((R)-1,1′-binaphthyl-2,2′-diyl)phosphite]-butane **2c**. Yield 68%. ^{1}H NMR (250 MHz): 8.01–7.72, 7.56–7.10 (m, 24 H, H2-H19), 4.07–3.80 (m, 2H, H22), 3.80–3.65 (m, 4H, H21), 1.33 (s, 6H, H24). ^{13}C{^{1}H} NMR (62.8 MHz): 147.3, 147.3 (4C, C1, C20); 133.0, 133.0 (4C, C9, C12); 131.5, 131.1 (4C, C3, C18); 130.9; 130.7 (4C, C4, C17); 128.8, 128.7 (4C, C5, C16); 127.4, 127.2 (4C, C7, C14); 126.8, 126.6 (4C, C6, C15); 125.6, 125.4 (4C, C8, C13); 123.1, 122.8 (4C, C10, C11); 122.3, 121.9 (4C, C2, C19); 110.6 (1C, C23); 78.7 (2C, C22); 64.1 (4C, C21); 27.4 (6C, C24). ^{31}P{^{1}H} NMR (101.3 MHz): 139.5 (s). $[\alpha]_D{}^{25} = -449.27^\circ$ ($c = 1.24$, CH_2Cl_2) FAB$^+$ MS: *m*/*z*: 791 [M+1]$^+$. TOF MS: *m*/*z*: 813.1787 (Calcd. 813.1777 for $C_{47}H_{37}O_8NaP_2{}^+$), error (ppm) = 1.1479.

2.3. Rhodium complexes: in situ NMR experiments

A NMR tube was charged under nitrogen with a $CDCl_3$ stock solution of [RhH(CO)(PPh_3)$_3$] (0.8 mL, 0.4 mmol) and the corresponding ligand (molar ratio diphosphite/Rh = 0.5). The solution was analyzed by ^{1}H and ^{31}P NMR and then was shaken at 25 °C during 1 h. After this time, the solution was analyzed again. The spectra were simulated by the gNMR software [27].

2.4. Palladium complexes

Complexes [Pd(η^3-allyl)(diphosphite)]PF_6 were prepared from [Pd(μ-Cl)(η^3-PhCHCHCHPh)]$_2$, NH_4PF_6, and the appropriate chiral diphosphite ligand according to a previously reported method [28].

[Pd(η^3-PhCHCHCHPh)(1a)]PF_6 (**9**). Yellow crystals (0.132 g, 72% yield). ^{1}H NMR (300 MHz) 1.19 (s, 9H), 1.50 (s, 9H), 1.55 (s, 9H), 1.62 (s, 9H), 3.04 (s, 3H), 3.10 (s, 3H), 3.36-3.51 (br m, 2H), 3.72 (s, 6H), 3.79 (s, 3H), 3.87 (s, 3H), 4.25–4.55 (br m, 2H), 4.85–5.10 (br m, 2H), 6.21 (m, 1H), 6.37–7.25 (m, 20 H). ^{31}P{^{1}H} NMR (121.4 MHz): 122.14 (s), −144.37 (sept, $^{1}J_{P\text{-}F} = 710.44$ Hz). FAB$^+$ MS: *m*/*z* 1221 [M]$^+$. HR-FAB$^+$ MS: *m*/*z*: 1221.4251 (Calcd. 1221.4233 for $C_{65}H_{81}O_{12}P_2Pd^+$), error (ppm) = 1.51.

[Pd(η^3-PhCHCHCHPh)(2a)]PF_6 (**10**). Yellow solid (0.126 g, 68% yield) ^{1}H NMR (300 MHz): 1.09–1.12 (m, 6H), 1.17 (m, 9H), 1.50 (m, 9H), 1.55 (m, 9H), 1.64 (m, 9H), 3.72 (s, 3H, major), 3.73 (s, 3H, minor), 3.80 (s, 3H, major), 3.88 (s, 3H, minor), 4.08 (br m, 4H), 5.07 (br m, 2H), 6.23 (br m, 1H), 6.48–7.22 (m, 20 H). ^{31}P{^{1}H} NMR (121 MHz): two isomers, major isomer: 122.40, 122.29; minor isomer: 121.22, 121.14, ratio 1.5:1; −143.90 (sept, $^{1}J_{P\text{-}F} = 708.46$). FAB$^+$ MS: *m*/*z*: 1233 [M]$^+$. HR-FAB$^+$ MS: *m*/*z*: 1233.4246 (Calcd. 1233.4233 for $C_{66}H_{81}O_{12}P_2Pd^+$), error (ppm) = 1.09.

2.5. Catalytic experiments

Hydroformylation experiments were carried out as previously reported [9]: [Rh(acac)(CO)$_2$] (6.4 mg, 0.025 mmol) and the appropriate amount of diphosphite in toluene (8 mL) was incubated at 30 bar of syn-gas and 60 °C for 2 h. A solution of styrene (1.2 mL, 10.0 mmol) in toluene (7 mL) was then added. The temperature was set and the autoclave was charged with syn-gas at working pressure. The conversion and regioselectivity were determined by GC analysis. The enantiomeric excess (*ee*) of the reaction was obtained by analyzing 2-phenylpropanal, as well as 2-phenylpropanoic acid, by a GC apparatus equipped with chiral columns (Supelco β-Dex 225 and β-Dex 120 chiral columns). Aldehydes were converted to the corresponding acids by a treatment with $KMNO_4/MgSO_4$ in acetone [4,29].

Allylic alkylation experiments were performed following previously reported methods [28]: [Pd(μ-Cl)(η^3-C_3H_5)]$_2$ (3.7 mg, 0.01 mmol) and the diphosphite ligand (0.025 mmol) in dichloromethane (1 mL) was stirred for 30 min. In some experiments, 200 or 400 μL of a CH_2Cl_2 stock solution of

Table 1
Hydroformylation of **S1** with [Rh(acac)(CO)$_2$]/diphosphite catalysts.[a].

Entry	L	% C (h)[b]	TOF[c]	%**4**	% ee **4**[d]
1	**1a**	79 (3)	109	93	4 (*S*)
2	**1b**	86 (24)	15	87	12 (*S*)
3	**1c**	98 (19)	21	89	10 (*R*)
4	**2a**	83 (4)	86	94	<2
5	**2b**	85 (24)	15	89	9 (*S*)
6	**2c**	95 (22)	18	89	10 (*R*)

[a] 0.25 mol% Rh: [Rh(acac)(CO)$_2$] = 1.66 mM, [L] = 2.08 mM mmol, toluene = 15 mL; P = 15 bar, $P_{CO} = P_{H_2}$, T = 40 °C, chemoselectivity was >99% in all cases.
[b] Conversion, time in parenthesis.
[c] TOF: turnover frequency calculated as average in the indicated time (h^{-1}).
[d] Absolute configuration of **4** is shown in parenthesis.

NaBAr'F (10 mM) were added. CH_2Cl_2 solutions (1 mL) of the substrate (1 mmol), dimethyl malonate (396 mg, 3 mmol) and *N*,*O*-bis(trimethylsilyl)acetamide (610 mg, 3 mmol) and 5 mg of KOAc were added. Aliquots were treated with diethyl ether, saturated aqueous ammonium chloride solution and filtered over silica using diethyl ether (**S2** and **S3**) or dichloromethane (**S4**) as eluents. The conversion and selectivity were determined by HPLC (Nucleocel Delta S) for **S2**, by HPLC (Chiralcel OJ-H) and GC (DB-WAX column) for **S3** and by GC (β-DEX 225 column) for **S4**.

3. Results and discussion

3.1. Syntheses of ligands

Diphosphites **1a–c** and **2a–c** were prepared by condensing the corresponding phosphorochloridites with the appropriate diol, in the presence of an excess of NEt_3 (Scheme 1). Ligands were purified from the small amounts of hydrolysis products formed during the reaction by passing a CH_2Cl_2 solution of the crude over activated silica. All diphosphites were fully characterized by conventional spectroscopic techniques. Because the C_2 symmetry of the ligands, their ^{13}C NMR show a single set of signals for one half of the diphosphite. However, it should be noticed that the local C_2 symmetry of the free biarylic groups is lost in the diphosphites. This produces slight differences on the chemical shift of equivalent carbons of the two moieties of each biarylic fragment (0.5–1 ppm).

The backbone of ligands type **2** has been only previously used in two reported diphosphites [13,30]. Other diphosphites derived from tartaric acid have been also described, but their structures are not related to those of ligands in Scheme 1 [31,32]. Diphosphites with the backbone of ligands **1a–c** have not been ever reported. Ligands **1a–c** and **2a–c** were applied in the metal-catalyzed reactions showed in Scheme 2.

3.2. Rhodium-catalyzed asymmetric hydroformylation

Screening catalytic experiments were carried out using styrene as substrate (**S1**, Scheme 2). Selected results are collected in Table 1.

The enantioselective discrimination achieved in the branched aldehyde **4** was low in all cases. Those containing binaphthyl fragment, **1b-c** and **2b-c**, produced *ee*'s around 10% with the two backbones used and the stereochemistry of the major aldehyde is controlled by the configuration of the binaphthyl fragment. Ligands **1b** and **2b** constructed with a (*S*)-binaphthol yield slight ee's on (*S*)-**4** (Table 1, entries 2 and 5), whereas similar ee's for (*R*)-**4** was obtained with ligands bearing a (*R*)-binaphthyl moiety (Table 1, entries 3 and 6). Therefore, there is not a cooperative effect between the chiral backbone and the binaphthyl fragments. Furthermore, ligands **1a** and **2a** with achiral biarylic fragment render meaningless ee's (Table 1, entries 1 and 4), but they are nearly ten times more active than the other four diphosphites with binaphthyl fragments.

Table 2
Pd-catalyzed allylic alkylation using ligands **1**-**2**.[a].

Entry	Substrate	L	% C (min)	**7/6**	% ee[b]
1	**S2**	**2a**	91 (3)		15 (*R*)
2	**S2**	**1a**	90 (15)		60 (*S*)
3[c]	**S2**	**1a**	45 (360)		68 (*S*)
4	**S2**	**1c**	100 (240)		14 (*R*)
5	**S2**	**1b**	55 (180)		10 (*R*)
6	**S3**	**1a**	100 (12)	46/54	5 (*R*)
7	**S3**	**2a**	100 (5)	49/51	8 (*R*)
8	**S3**	**2b**	54 (240)	27/73	15 (*R*)
9	**S3**	**2c**	100 (90)	9/91	20 (*R*)
10	**S3**	**1b**	53 (240)	49/51	16 (*R*)
11	**S4**	**1a**	100 (15)		28 (*R*)
12	**S4**	**2a**	100 (15)		5 (*R*)
13	**S4**	**1b**	10 (120)		25 (*R*)

[a] 2 mol% Pd: [Pd(π-C_3H_5)Cl]$_2$ = 2.5 mM, [L] = 6.25 mM, [KOAc] = 12.7 mM, [Substrate]:[CH_2(COOMe)$_2$]:[BSA] = 1:3:3, CH_2Cl_2 = 4 mL.
[b] Absolute configuration of products is shown in parenthesis.
[c] Carried out at −40 °C.

The regioselectivities attained with **1a** and **2a** in the branched aldehyde **4** were higher (93–94%) than those obtained with ligands **1b-c** and **2b-c** (84–90%).

3.3. Palladium-catalyzed asymmetric allylic alkylation reactions

Ligands **1**-**2** were screened in the palladium-catalyzed asymmetric allylic alkylation of *rac*-1,3-diphenyl-3-acetoxyprop-1-ene (**S2**), 1-phenyl-3-acetoxyprop-1-ene (**S3**), and *rac*-3-acetoxycyclohexene (**S4**) with dimethyl malonate as nucleophile and BSA as base (Scheme 2). Table 2 shows selected catalytic data for alkylation reactions of these substrates.

The Pd/**2a** system is the most active of all catalysts tested (Table 2, entry 1). Given the high activity of this system at 2 mol% Pd in the alkylation of **S2**, experiments at 0.1, 2×10^{-2} and 1×10^{-2} mol% were carried out and TOF's of 2220, 6000 and 7200 h^{-1} were achieved, respectively. The ee's in the (*R*)-**5** product were around 15% in all cases and they do not significantly enhance by lowering the temperature. Activities achieved with the Pd/**2a** are among the highest reported for asymmetric allylic alkylation [15]. Although the catalytic system Pd/**1a** is also fairly active, the rates achieved were lower than those of Pd/**2a** (Table 2, entry 2). Besides, the best asymmetric induction (*ca.* 70% in (*S*)-**5**) was achieved with ligand **1a** (Table 2, entry 3) in spite that the backbone of this ligand is more flexible than that of **2a**. It is also noteworthy that in these cases, the configurations of major enantiomer of **5** are opposite. Recently, it was reported a positive effect of the B[3,5-$(CF_3)_2C_6H_3]_4^-$ (BAr'F) counterion on the enantioselectivity of the allylic alkylation of **S2** [33]. Nonetheless, in our case, attempts to improve the steroselectivity of the system Pd/**1a** by adding Na(BAr'F) to the catalytic reaction were unsuccessful.

Catalysts with ligands **1b-c** and **2b-c**, bearing binaphthyl moieties, provided lower activities than **1a** and **2a** and poorer enantiomeric excesses (*ca.* 15%) in the alkylation of **S2**. Thus, the presence of the atropoisomeric fragment has a detrimental effect on both, the asymmetric induction and the activity of the catalyst, although the later effect is more remarkable. These results contrast with those reported in the same reaction for diphosphoroamidite, phosphite-phosphoroamidite and phosphite-oxazoline palladium catalysts, where the use of binaphthyl moieties instead of substituted biphenyls improves the enantioselectivity [34–36].

The allylic alkylation of **S3** leads to the formation of linear and branched isomers (**6** and **7**), depending on the terminal allylic carbon attacked by the nucleophile (Scheme 2). In palladium-catalyzed asymmetric alkylation of mono-substituted

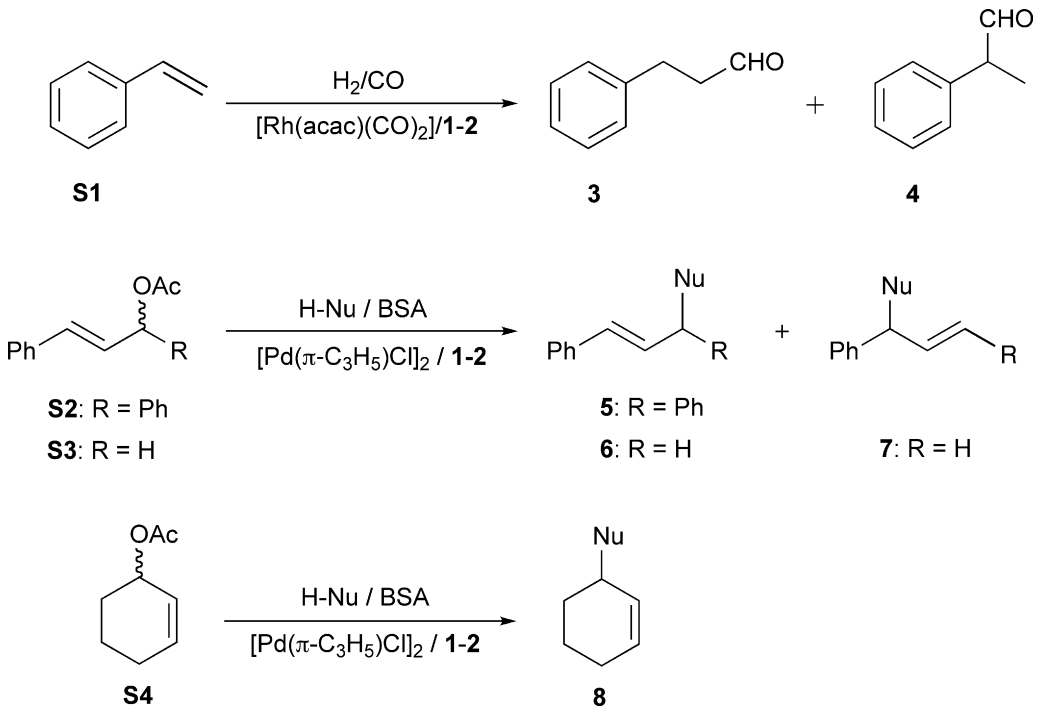

Scheme 2. Rhodium-catalyzed asymmetric hydroformylation and palladium-catalyzed asymmetric allylic alkylation reactions.

linear substrates like **S3**, low regioselectivies are often reported, since in most cases the achiral linear isomer **6** is favored rather than the desired chiral branched isomer **7** [37–39]. Ligand **1a** showed good activity, moderated regioselectivity and low enantioselectivity with this substrate (Table 2, entry 6). When the flexible backbone of **1a** was replaced by the stiffer one of **2a**, the rate of the reaction increased and the selectivity remains nearly the same (Table 2, entry 7). Further improvement on the turnover frequency (TOF = 1440 h^{-1}) was achieved with a lower catalyst load (0.1 mol% Pd). This is the highest rate reported for the allylic alkylation of **S3** catalyzed by palladium/diphosphite system. Moreover, regioselectivities in the branched product **7** (*ca.* 50%) achieved with **1a** and **2a** are the highest reported using a diphosphite ligand. Both, the activity and the regioselectivity of the catalyst significantly decreased when the biphenyl fragment in ligand **2a** was replaced by a binaphthyl one, ligands **2b** and **2c**, although the ee's slightly increased (Table 2, entries 8 and 9 *vs.* 7). Low-temperature experiments with **S3** were carried out, but the ee's remained almost invariable.

Diphosphites were also tested in alkylation of *rac*-3-acetoxycyclohexene (**S4**) (Scheme 2, Table 2). The asymmetric allylic alkylation of cyclic substrates is a difficult process due to the presence of less sterically demanding *syn* substituents, which often results in a low asymmetric induction. General trends observed in the allylic alkylation of **S2** and **S3** were reproduced with **S4**. Ee's in the product (*R*)-**8** were below 30%. The highest activities were achieved with **1a** and **2a**. For **2a**, the reaction was also accomplished at a low catalyst concentration (0.1 mol% Pd), affording a high rate for substrate **S4** (TOF = 225 h^{-1}).

During the alkylation of **S2** with the catalyst Pd/**1a**, a kinetic resolution of this substrate was observed. The unreacted substrate was steadily enriched in the (*S*)-isomer along the reaction (Fig. 1), while the ee of the product **5** remained unchanged. After 15 min (*ca.* 90% conversion), enantioselectivities of 99% for (*S*)-**S2** and 60% for (*S*)-**5** were attained at 20 °C.

Table 3 shows selected data obtained for the kinetic resolution of **S2** at different temperatures, providing also the *s* parameter (defined as the ratio k_R/k_S or k_{rel}) in order to asses the effect of the temperature on the relative reaction rates of the two enantiomers of the substrate. It should be noted that these values were calculated considering a first-order kinetic dependence for the substrate in the reaction rate. However, the kinetic dependence of the substrate can vary during the reaction course, leading to inaccurate estimations of the *s* values [40]. Indeed, it was observed

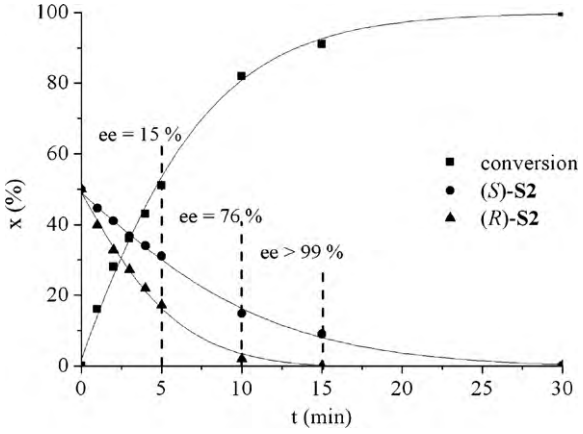

Fig. 1. Kinetic resolution of **S2** using chiral diphosphite ligand **1a** at 20 °C. Reaction conditions are indicated in Table 3.

Table 3
Kinetic resolution of **S2** using ligand **1a**.[a]

Entry	*T* (°C)	% C (min)	% ee **S2**[b]	% ee **5**[b]	*s*[c]
1	20	28 (2)	9 (*S*)	60 (*S*)	1.7
2	20	36 (3)	15 (*S*)	60 (*S*)	2.0
3	20	90 (15)	>99 (*S*)	60 (*S*)	n.d.
4	0	28 (10)	30 (*S*)	63 (*S*)	10.4
5	−40	30 (180)	32 (*S*)	68 (*S*)	9.4

[a] For reaction conditions see Table 2.
[b] Absolute configurations of **S2** and **5** are shown in parentheses.
[c] $s = k_R/k_S = \ln[(1 - C/100)(1 - ee/100)]/\ln[(1 - C/100)(1 + ee/100)]$
(*C* = conversion; ee = ee of **S2**), n.d. = not determined.

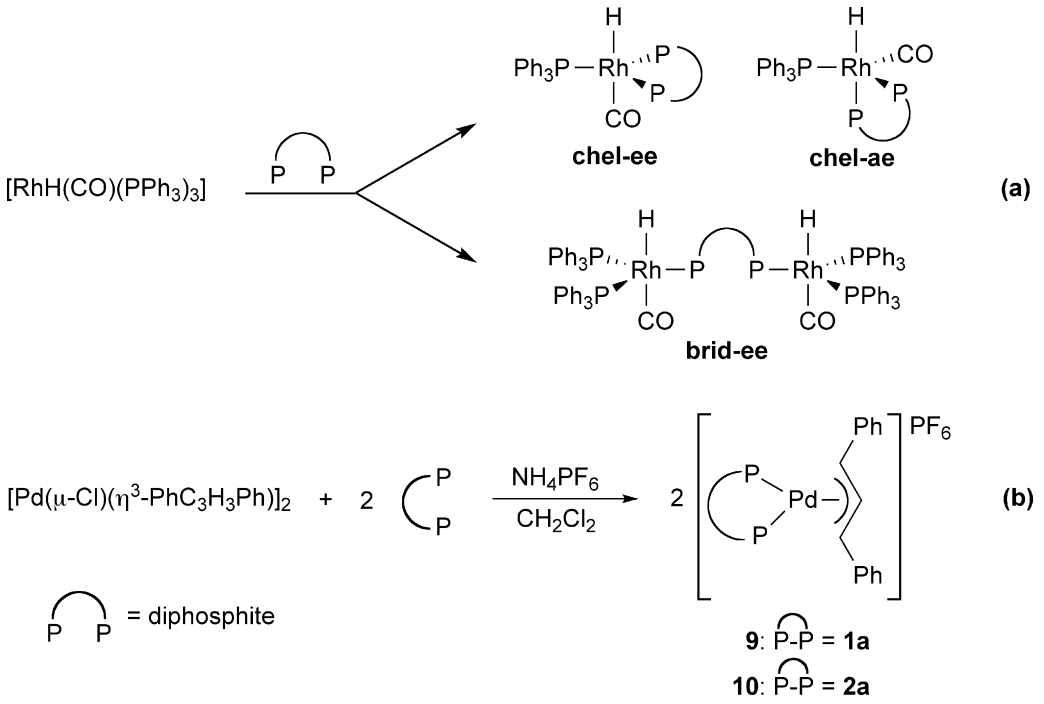

Scheme 3. Rhodium and palladium complexes. (a) Hydrido-carbonyl rhodium species. (b) Allyl-palladium active species.

that the calculated values changed with the conversion (Table 3, entries 1–3). The inspection of the *s* factors at similar conversions indicates that the racemic resolution is enhanced when the temperature is lowered from 20 °C to 0 °C, but no further improvement was observed at −40 °C. The substrate was recovered in low yields (10–15%) with ee's > 99% (*S*) and 90% (*S*), at 20 °C and 0 °C, respectively. Because the ee of the product **5** is the same throughout the reaction course, both enantiomers of **S2** must lead to the same cationic catalytic intermediate or if several species are formed, they have to be involved in fast equilibria [41].

3.4. Coordination properties

Evidence about the coordinating properties of diphosphites **1**–**2** was gathered by exploring the structure of complexes formed in the reactions of these ligands with $[RhH(CO)(PPh_3)_3]$ and $[Pd(\mu\text{-}Cl)(\eta^3\text{-}PhCHCHCHPh)]_2$. Complexes generated are related to the catalytic species in hydroformylation and allylic alkylation respectively.

The reaction of $[RhH(CO)(PPh_3)_3]$ with bidentate P-donor ligands is a useful probe to test their chelating properties [9,42]. Ligands with low tendency to produce chelates form species type **brid-ee** (other isomers are also possible), while ligands that are

Table 4
NMR data for hydrido-carbonyl rhodium species with ligands **1a-c** and **2a-c**.[a]

Ligand	Species	δ (ppm) phosphine	δ (ppm) phosphite	δ (ppm) hydride	*J* (Hz)
1a	brid-ee	P1: 34.1 P2: 36.2	P3: 151.4	−9.91 Broad	$^1J_{Rh\text{-}P1} = {}^1J_{Rh\text{-}P2} = 148.9$; $^1J_{Rh\text{-}P3} = 265.4$; $^2J_{P1\text{-}P2} = 93.7$; $^2J_{P1\text{-}P3} = {}^2J_{P2\text{-}P3} = 180.2$
1b[b]	brid-ee	P1: 37.4 P2: 40.3	P3: 175.8	−10.03 Broad	$^1J_{Rh\text{-}P1} = 143.5$; $^1J_{Rh\text{-}P2} = 147.7$; $^1J_{Rh\text{-}P3} = 259.5$; $^2J_{P1\text{-}P2} = 86.3$, $^2J_{P1\text{-}P3} = 194.9$; $^2J_{P2\text{-}P3} = 167.5$;
1b	chel-ee	P1: 32.9	P2: 158.1 P3: 171.6	−10.30 Broad	$^1J_{Rh\text{-}P1} = 152.7$; $^1J_{Rh\text{-}P2} = 244.4$; $^1J_{Rh\text{-}P3} = 256.5$; $^2J_{P1\text{-}P2} = 122.8$; $^2J_{P1\text{-}P3} = 153.1$; $^2J_{P2\text{-}P3} = 326.2$
1c	brid-ee	P1: 44.3 P2: 47.2	P3: 181.0	−9.90	$^1J_{Rh\text{-}P1} = 149.4$; $^1J_{Rh\text{-}P2} = 146.6$; $^1J_{Rh\text{-}P3} = 256.4$; $^2J_{P1\text{-}P2} = 88.5$; $^2J_{P1\text{-}P3} = 183.2$; $^2J_{P2\text{-}P3} = 192.3$; $^2J_{H\text{-}P1/2/3} = 8.0$; $^1J_{H\text{-}Rh} = 9.5$
2a	chel-ee + brid-ee	P1: 32.4 P1: 34.2 P2: 37.2	P2: 120.9 P3: 123.0 P3: 147.3	−10.28 Broad −9.94 Broad	$^1J_{Rh\text{-}P1} = 136.6$; $^1J_{Rh\text{-}P2} = 244.1$; $^1J_{Rh\text{-}P3} = 270.4$; $^2J_{P1\text{-}P2} = 101.3$; $^2J_{P1\text{-}P3} = 161.7$; $^2J_{P2\text{-}P3} = 199.9$ $^1J_{Rh\text{-}P1} = 146.5$; $^1J_{Rh\text{-}P2} = 148.3$; $^1J_{Rh\text{-}P3} = 265.9$; $^2J_{P1\text{-}P2} = 85.8$; $^2J_{P1\text{-}P3} = {}^2J_{P2\text{-}P3} = 179.5$
2b[b]	brid-ee	P1: 37.4 P2: 40.1	P3: 175.3	−9.87 Broad	$^1J_{Rh\text{-}P1} = 143.8$; $^1J_{Rh\text{-}P2} = 147.6$; $^1J_{Rh\text{-}P3} = 259.4$; $^2J_{P1\text{-}P2} = 86.3$; $^2J_{P1\text{-}P3} = 168.6$; $^2J_{P2\text{-}P3} = 190.6$
2b	chel-ee	P1: 32.0	P2: 164.2 P3: 169.7	−10.53 Broad	$^1J_{Rh\text{-}P1} = 139.7$; $^1J_{Rh\text{-}P2} = 240.0$; $^1J_{Rh\text{-}P3} = 240.0$; $^2J_{P1\text{-}P2} = 117.5$; $^2J_{P1\text{-}P3} = 140.4$; $^2J_{P2\text{-}P3} = 240.0$
2c	chel-ee	P1: 35.8	P2: 173.9 P3: 177.4	−9.99	$^1J_{Rh\text{-}P1} = 137.3$; $^1J_{Rh\text{-}P2} = 238.1$; $^1J_{Rh\text{-}P3} = 247.2$; $^2J_{P1\text{-}P2} = 128.2$; $^2J_{P1\text{-}P3} = 143.5$; $^2J_{P2\text{-}P3} = 289.0$; $^2J_{H\text{-}P1} = 7.7$, $^2J_{H\text{-}P2/3} = 9.0$, $^1J_{H\text{-}Rh} = 8.7$

[a] After 1 h of reaction at 25 °C, [L]/[Rh] = 0.5 in $CDCl_3$.
[b] After 15 min of reaction.

prone to form a chelate complex render species type **chel-ee** or **chel-ae**, depending on the bite angle of the ligand (Scheme 3a) [43]. The three species are easily distinguished by NMR, providing a simple diagnostic for the chelating properties of new ligands. Table 4 collects the results of ^{31}P and the hydride region of the ^{1}H NMR spectra for the species formed in this reaction.

^{31}P NMR spectra display two set of signals corresponding to coordinated phosphine and phosphite around 40 and 180 ppm respectively. In the case of ligands **1a** and **1c**, the phosphine signals integrate twice respect to those assigned to phosphite, which is consistent with a phosphite bridge between two [RhH(CO)(PPh_3)$_2$] fragments. The high $J_{P\text{-}P}$ values (>85 Hz) and small coupling values between P and H ligands (*ca.* 10 Hz) indicate that the three P-donor ligands occupy equatorial positions and that they are *cis* respect to the hydride. These observations are in agreement with a structure type **brid-ee** for these species. Similar behavior was found by ligand **2a**, although it partially evolves to a **chel-ee** species (*ca.* 2:1 **brid-ee**:**chel-ee**) producing a stable mixture of species. In contrast, ligand **2c** forms a **chel-ee** species for the complex [RhH(CO)(PPh_3)(**2c**)]. The integration of the phosphite region is twice that of the phosphine, the values of all $J_{P\text{-}P}$ are high (>100 Hz) and P-H coupling constants are below 10 Hz. These facts are compatible with a **chel-ee** structure. Similar behavior was observed for Rh/**1b** and Rh/**2b** species, but **brid-ee** species were formed at the first stages of the reaction. After 1 h at room temperature, binuclear complexes evolve to **chel-ee** species in both cases.

Palladium complexes [Pd(η^3-PhCHCHCHPh)(diphosphite)]PF_6, **9** and **10** were prepared in order to understand the different behavior displayed in allylic alkylation of **S2** (Scheme 3b). Structural studies in solution by NMR experiments, revealed the presence of only one isomer for **9** and two diastereomeric species in relative ratio 1.5:1 at 298 °C for **10**. These isomers can be assigned to the M- and W-type allylic species which are involved in a interchange equilibrium *via* π–σ–π mechanism [44,45]. Furthermore, the C_2-symmetry of **1a** and **2a** diphosphites when they are coordinated to the metal is broken, since four set of signals for *tert*-butyl groups were observed. The presence of only one isomer for complex **9** could explain the better asymmetric induction displayed for the catalytic system Pd/**1a**, when compared with the results obtained with ligand **2a**.

4. Conclusions

A series of diphosphite ligands were easily prepared from a backbone obtained from tartaric acid. These ligands were tested in Rh-catalyzed hydroformylation and Pd-catalyzed allylic alkylation reactions. Albeit ligands **1b** and **2b-c** form equatorial-equatorial chelates in rhodium-hydrido pentacoordinated species, the chiral pocket generated by these ligands does not seem appropriated to attain high enantiodiscrimination in the styrene hydroformylation. Low *ee's* were obtained with all diphosphites and no matching effect was observed between tartaric-derived backbone and binaphthyl substituents at phosphite moieties. High activities were achieved with ligands **1a** and **2a**, containing bulky bisphenyl groups.

In allylic alkylation reactions, Pd/**2a** system showed very high rates for the disubstituted linear substrate **S2** (TOF = 7200 h^{-1}), the mono-substituted linear substrate **S3** (TOF = 1440 h^{-1}) and the cyclic substrate **S4** (TOF = 225 mol h^{-1}). These activities are among the highest in Pd-catalyzed allylic substitutions reactions for these substrates. In spite of the low enantioselectivity, the selectivity obtained in the branched isomer **7** arising from **S3** was fairly good (*ca.* 50%). Furthermore, a kinetic resolution of **S2** was observed during the alkylation of this substrate with Pd/**1a**. Ee values higher than 99% for the unreacted substrate (*S*)-**S2** and 68% (*S*) for the alkylated product **5** were achieved. To sum up, the excellent activities of the Pd systems with ligands **1a** and **2a** can be highlighted. Both ligands share the presence of substituted biphenyl moieties, although the stiffness of their backbone is remarkable different. The difference in the stereoselectivity of these two ligands in alkylation reactions can arise from the fact that, in solution, only one isomer was detected for the cationic allylic species [Pd(η^3-PhCHCHCHPh)(**1a**)]$^+$, while two isomers were observed for [Pd(η^3-PhCHCHCHPh)(**2a**)]$^+$.

Acknowledgements

The authors thank Conacyt-Mexico CB-060430 and CB-060894, Dgapa-UNAM IN210607 and Spanish DGI through project (CTQ2005-09187-C02-01) for the financial support and CYTED (Project V9) for a bursary to E. Vargas-Malvaez.

Appendix A. Supplementary data

Supplementary data associated with this article can be found, in the online version, at doi:10.1016/j.molcata.2010.06.001.

References

[1] C. Claver, O. Pàmies, M. Diéguez, in: A. Borner (Ed.), Phosphorous Ligands in Asymmetric Catalysis, Wiley-VCH, Weinheim, 2008, pp. 506–528.
[2] J. Klosin, C.R. Landis, Acc. Chem. Res. 40 (2007) 1251–1259.
[3] M. Diéguez, O. Pàmies, Acc. Chem. Res. 43 (2010) 312–322.
[4] J.E. Babin, G.T. Whiteker, PCT Int. Appl., WO 93/03839 for Union Carbide (1993).
[5] G.J.H. Buisman, E.J. Vos, P.C.J. Kamer, P.W.N.M. van Leeuwen, J. Chem. Soc., Dalton Trans. (1995) 409–417.
[6] M. Diéguez, O. Pàmies, C. Claver, Chem. Commun. (2005) 1221–1223.
[7] J. Mazuela, M. Coll, O. Pàmies, M. Diéguez, J. Org. Chem. 74 (2009) 5440–5445.
[8] C.J. Cobley, J. Klosin, C. Qin, G.T. Whiteker, K.A. Abboud, Organometallics 26 (2007) 2986–2999.
[9] Z. Freixa, J.C. Bayón, J. Chem. Soc., Dalton Trans. 14 (2001) 2067–2068.
[10] M. Diéguez, S. Jansat, M. Gómez, A. Ruiz, G. Muller, C. Claver, Chem. Commun. (2001) 1132–1133.
[11] O. Pàmies, G.P.F. van Strijdonck, M. Diéguez, S. Deerenberg, G. Net, A. Ruiz, C. Claver, P.C.J. Kamer, P.W.N.M. van Leeuwen, J. Org. Chem. 66 (2001) 8867–8871.
[12] M. Diéguez, A. Ruiz, C. Claver, Dalton Trans. (2003) 2957–2963.
[13] M. Diéguez, O. Pàmies, C. Claver, J. Org. Chem. 70 (2005) 3363–3368.
[14] M. Diéguez, O. Pàmies, C. Claver, Adv. Synth. Catal. 347 (2005) 1257–1266.
[15] A. Castillo, I. Favier, E. Teuma, S. Castillón, C. Godard, A. Aghmiz, C. Claver, M. Gómez, Chem. Commun. (2008) 6197–6199.
[16] A. Marson, Z. Freixa, P.C.J. Kamer, P.W.N.M. van Leeuwen, Eur. J. Inorg. Chem. 29 (2007) 4587–4591.
[17] J. Wilting, M. Janssen, C. Müeller, M. Lutz, A. Spek, D. Vogt, Adv. Synth. Catal. 349 (2007) 350–356.
[18] Y. Zou, Y. Yan, X. Zhang, Tetrahedron Lett. 48 (2007) 4781–4784.
[19] D. Sanhes, A. Gual, S. Castillón, C. Claver, M. Gómez, E. Teuma, Tetrahedron: Asymmetry 20 (2009) 1009–1014.
[20] M.R. Axet, J. Benet-Buchholz, C. Claver, S. Castillón, Adv. Synth. Catal. 349 (2007) 1983–1998.
[21] D. Seebach, H.-O. Kalinowski, B. Bastani, G. Crass, H. Daum, H. Dörr, N.P. Dupreez, V. Ehrig, W. Langer, C. Nüssler, H.-A. Oei, M. Schmidt, Helv. Chim. Acta 60 (1977) 301–325.
[22] K. Mori, Tetrahedron 30 (1974) 4223–4227.
[23] P.W. Feit, J. Med. Chem. 7 (1964) 14–17.
[24] T. Jongsma, M. Fossen, G. Challa, P.W.N.M. van Leeuwen, J. Mol. Catal. 83 (1993) 17–35.
[25] G.J.H. Buisman, P.C.J. Kamer, P.W.N.M. van Leeuwen, Tetrahedron: Asymmetry 4 (1993) 1625–1634.
[26] R. Brindaban, D. Suvendu, H. Alakananda, Green Chem. 5 (2003) 44–46.
[27] gNMR Simulation program, P.H.M. Budzelaar, version 5.0, Ivory Soft.
[28] F. Fernández, M. Gómez, S. Jansat, G. Muller, E. Martin, L. Flores-Santos, P.X. García, A. Acosta, A. Aghmiz, M. Jiménez, A. Masdeu-Bultó, M. Diéguez, C. Claver, M.A. Maestro, Organometallics 24 (2005) 3946–3956.
[29] L. Crespi, Ph.D. thesis, Universitat Autònoma de Barcelona, 2007.
[30] H. Brunner, W. Zettlmeier, Bull. Soc. Chim. Belg 100 (1991) 247–257.
[31] S.B. Owens Jr., G.M. Gray, Organometallics 27 (2008) 4282–4287.
[32] S.-H. Kyung, C.-H. Kim, Agric. Chem. Biotechnol. 46 (2003) 156–159.
[33] L.A. Evans, N. Fey, J.N. Harvey, D. Hose, G.C. Lloyd-Jones, P. Murray, A.G. Orpen, R. Osborne, G.J.J. Owen-Smith, M. Purdie, J. Am. Chem. Soc. 130 (2008) 14471–14473.
[34] E. Raluy, M. Diéguez, O. Pàmies, J. Org. Chem. 72 (2007) 2842–2850.
[35] O. Pàmies, M. Diéguez, Chem. Eur. J. 14 (2008) 944–960.
[36] M. Diéguez, O. Pàmies, Chem. Eur. J. 14 (2008) 3653–3669.
[37] R. Prétôt, A. Pfaltz, Angew. Chem. Int. Ed. 37 (1998) 323–325.
[38] R. Hilgraf, A. Pfaltz, Synlett (1999) 1814–1817.

[39] S.-L. You, X.-Z. Zhu, Y.-M. Luo, X.-L. Hou, L.-X. Dai, J. Am. Chem. Soc. 123 (2001) 7471–7472.
[40] J.M. Keith, J.F. Larrow, E.N. Jacobsen, Adv. Synth. Catal. 343 (2001) 5–26.
[41] S. Ramdeehul, P. Dierkes, R. Aguado, P.C.J. Kamer, P.W.N.M. van Leeuwen, J.A. Osborn, Angew. Chem. Int. Ed. 37 (1998) 3118–3121.
[42] Z. Freixa, M.M. Pereira, A.A.C.C. Pais, J.C. Bayón, J. Chem. Soc., Dalton Trans. (1999) 3245–3251.
[43] P.W.N.M. van Leeuwen, P.C.J. Kamer, J.N.H. Reek, P. Dierkes, Chem. Rev. 100 (2000) 2741–2769.
[44] G. Helmchen, U. Kazmaiel, S. Forster, in: I. Ojima (Ed.), Catalytic Asymmetric Synthesis, third ed., John Wiley & Sons, Hoboken, 2010, pp. 497–641.
[45] A.M. Masdeu-Bultó, M. Diéguez, E. Martin, G. Gómez, Coord. Chem. Rev. 242 (2003) 159–201.